

# Phase matching characteristics of deuterated ammonium dihydrogen phosphate crystals

Lili Zhu (朱丽丽)<sup>1,2</sup>, Baoan Liu (刘宝安)<sup>1,2</sup>, Lisong Zhang (张立松)<sup>1,2</sup>,  
Qinghua Zhang (张清华)<sup>3</sup>, Zhengping Wang (王正平)<sup>1,2</sup>, and Xun Sun (孙洵)<sup>1,2,\*</sup>

<sup>1</sup>State Key Laboratory of Crystal Materials, Shandong University, Jinan 250100, China

<sup>2</sup>Key Laboratory of Functional Crystal Materials and Device, Shandong University,  
Ministry of Education, Jinan 250100, China

<sup>3</sup>Chengdu Fine Optical Engineering Research Center, Chengdu 610041, China

\*Corresponding author: sunxun@sdu.edu.cn

Received December 7, 2014; accepted January 28, 2015; posted online March 17, 2015

Refractive indices for crystals ammonium dihydrogen phosphate (ADP), 30% deuterated ADP (DADP), 50% DADP, and 70% DADP are measured from 253 to 1529 nm with  $5 \times 10^{-6}$  accuracy. Numerical fits to modified double-pole Sellmeier equation are made. Second-harmonic generation, third-harmonic generation phase matching (PM) angles, and noncritical PM (NCPM) wavelengths are calculated using the Sellmeier parameters. The deuterated crystals show smaller PM angles than pure crystal. Fourth-harmonic generation process can be realized by DADP in smaller deuterium content than deuterated potassium dihydrogen phosphate (DKDP). The measured NCPM wavelengths are consistent with the calculated value. PM characteristics are compared between DADP and DKDP.

OCIS codes: 160.4760, 160.4330, 260.1180, 190.4400.

doi: 10.3788/COL201513.041601.

Potassium dihydrogen phosphate (KDP) and partially deuterated KDP (DKDP) are two well-known nonlinear optical materials used as electro-optic switches and frequency conversion crystals in high-power laser systems<sup>[1,2]</sup>. As an important isomorph of KDP, ammonium dihydrogen phosphate (ADP) has also been well studied. Compared with KDP crystal, ADP has a larger nonlinear optical coefficient, and a higher conversion efficiency and laser damage threshold<sup>[3-6]</sup>. Studies on deuterated ADP (DADP) crystals showed that DADP crystal can effectively decrease the spontaneous Raman scattering intensity and realize the noncritical phase matching (NCPM) process of 526→263 nm at room temperature<sup>[7-9]</sup>. For 60% DADP crystal, the performance in NCPM fourth-harmonic generation (FHG) angular bandwidth, output energy, and conversion efficiency are also better than 70% DKDP<sup>[9]</sup>. All these studies demonstrated that DADP is a prospective crystal that can play important role in the area of second-harmonic generation (SHG), third-harmonic generation (THG), and FHG.

The alteration of deuterium content can effectively change the optical properties. For DKDP crystals, deuteration can decrease the refractive indices and hence change the phase matching (PM) angles and wavelength<sup>[10]</sup>. While the efficient PM is important in many phase-sensitive nonlinear processes, especially in parametric processes like harmonic generation, parametric amplification, and oscillation, as well as four-wave mixing. In the process of frequency harmonic or optical parametric amplification, PM needs to be achieved to ensure a high conversion efficiency<sup>[11-14]</sup>. For better application of DADP crystals in PM area, we should study its dependent on

deuterium content. Thus the accurate measurements of refractive indices for DADP crystals with different deuterium content are inevitably needed. The refractive indices of KDP and ADP in the whole transmission region were first measured by Zernike<sup>[15]</sup> at 298 K. Subsequent measurements for KDP isomorphs<sup>[16,17]</sup> were limited in visible region that does not span to the absorption edge. The temperature dependence of the indices for ADP was also measured within different temperature and wavelength region<sup>[18-20]</sup>. But the thermo-optic coefficients are still hard to determine.

The purpose of this work is to give accurate values of refractive indices for DADP crystals that spanning the entire range of transparency. Based on the dependence of refractive indices on deuterium concentration, the variation of PM characteristics can also be determined. The calculated NCPM wavelengths were consistent with the experimental value, which proved the accuracy of the measurements and fitting. This work will provide good references for the nonlinear optical applications of DADP crystals.

DADP crystals are grown from aqueous solution by the traditional temperature-reduction method. The solutions are made by dissolving extra-pure  $\text{NH}_4\text{H}_2\text{PO}_4$  salt into heavy water and deionized water with the resistivity of  $18 \text{ M}\Omega \cdot \text{cm}$ . Filtration with  $0.22 \mu\text{m}$  microporous membrane is made before the overheating of solution. The  $5 \text{ cm} \times 5 \text{ cm} \times 1 \text{ cm}$   $z$ -cut seed is also overheated before putting into the solution. Crystallization is performed in the temperature range of 308–323 K and the growth rate is approximately 1 mm/day for all the crystals. These crystals have no visible macroscopic defect.

Right-angle prisms are cut from the crystals above, as shown in Fig. 1.

The measurement principle of refractive indices is based on the minimum deviation method, as shown in Fig. 2. A bundle of monochromatic collimated light enters vertically at the larger right-angle surface (parallel to the optic axis direction) and is refracted at the second surface when leaving the crystal. Using

$$n = \frac{\sin \theta}{\sin \delta}, \quad (1)$$

where  $\theta$  is the refraction angle, and  $\delta$  the incidence angle (also the apex angle of the prism), the refractive index  $n$  can be obtained.

The measuring instrument is HR SpectroMaster UV-visible-IR from Trioptics company, with the measuring accuracy of  $5 \times 10^{-6}$ . The refractive indices at each wavelength are measured 6 times to ensure the accuracy of the values. Since DADP crystals are negative uniaxial crystals, the ordinary index of refraction ( $n_o$ ) is higher than the extraordinary index of refraction ( $n_e$ ). A dryer and a dehumidifier are used to assure dryness of the samples before and during the measurements. The test temperature is 302 K with the fluctuation of 0.5 K. The data spans the region from 253 to 1529 nm.

The optical transmittance spectra was measured by a spectrophotometer (Model U-3500, Hitachi) in the range of 200–2000 nm, as shown in Fig. 3. The IR absorption edge of DADP crystals increases with the deuterium content. Deuterated ADP crystals are also more transparent in the near-IR region than pure ADP. But it is obvious that the transmittance of pure ADP is higher than that

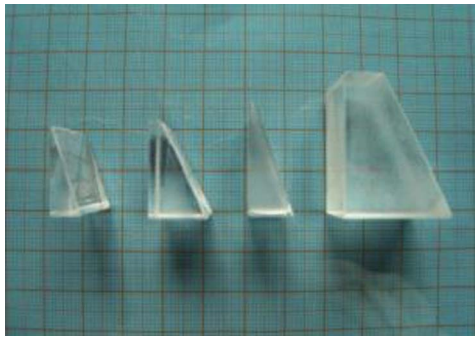


Fig. 1. Samples cut from the traditionally grown crystals.

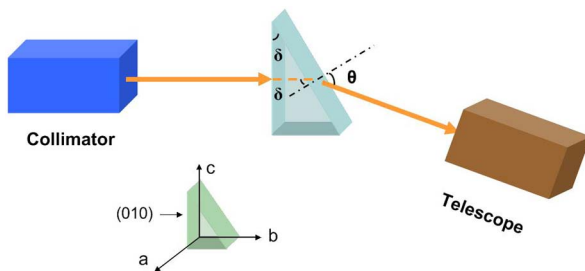


Fig. 2. Measurement principle of refractive index.

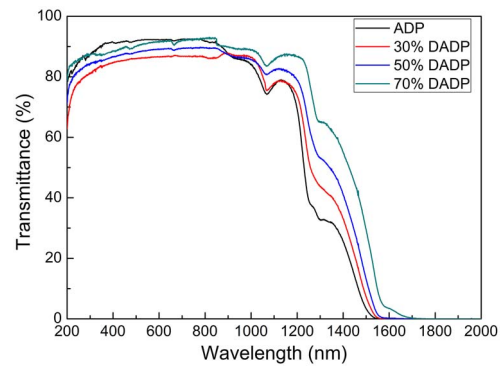


Fig. 3. Transmittance spectra of DADP crystals.

of DADP in the UV region. The absorption in the IR transmission spectrum is believed to be overtone of O-H absorption band, which is sensitive to the level of deuteration<sup>[17]</sup>. Thus the IR edge can be red shifted after deuteration. The absorption band between 1000 and 1100 nm is believed to be an overtone of N-H absorption band, which is weakened after deuteration. The absorption between 200 and 400 nm<sup>[21]</sup> can be attributed to the presence of impurity.

KDP has a better transmittance behavior than ADP in the near-IR, and contributes to the popularity of KDP crystal on large laser aperture system<sup>[20]</sup>. After deuteration of ADP, DADP crystals have higher transmittance in this region and larger IR adsorption edge, which is comparable to KDP crystal. The IR absorption edge of KDP crystal is about 1680 nm while that of 70% DADP is about 1740 nm. This can greatly improve the usefulness of DADP crystals as optical devices.

The variation of refractive indices with wavelength is shown in Fig. 4. The refractive indices decrease with the increasing wavelength and deuterated content. The difference of changing tendency between  $n_o$  and  $n_e$  is that  $n_o$  increases after deuteration while  $n_e$  rarely changes at 1529 nm. The birefringence ( $n_o - n_e$ ) of DADP crystals is shown in Fig. 5. Kirby and DeShazer's<sup>[16]</sup> data of 96% DADP is also added into Fig. 5. Deuteration lowered the birefringence at most wavelengths but enhanced it at 1529 nm, due to the different trend of  $n_o$  and  $n_e$ . The data from Kirby is consistent with our changing tendency.

Comparison of refractive indices for KDP and ADP is shown in Fig. 6. It is obvious that the indices of ADP are higher than KDP. In fact, isomorphs with  $\text{NH}_4^+$  groups consistently have higher indices than the respective  $\text{K}^+$  crystals in both the deuterated and the undeuterated cases.

Birefringence is an important optical parameter for electro-optical functional materials, and is mainly determined by the anisotropy of crystal. Though the anisotropy of lattice constant for ADP is obviously smaller than KDP, the birefringence of ADP is larger than KDP. Probably due to that  $\text{NH}_4^+$  has a relatively large polarizability<sup>[22]</sup>. Large birefringence can obtain a wider tuning range, which is helpful in the application of optical parametric oscillator (OPO).

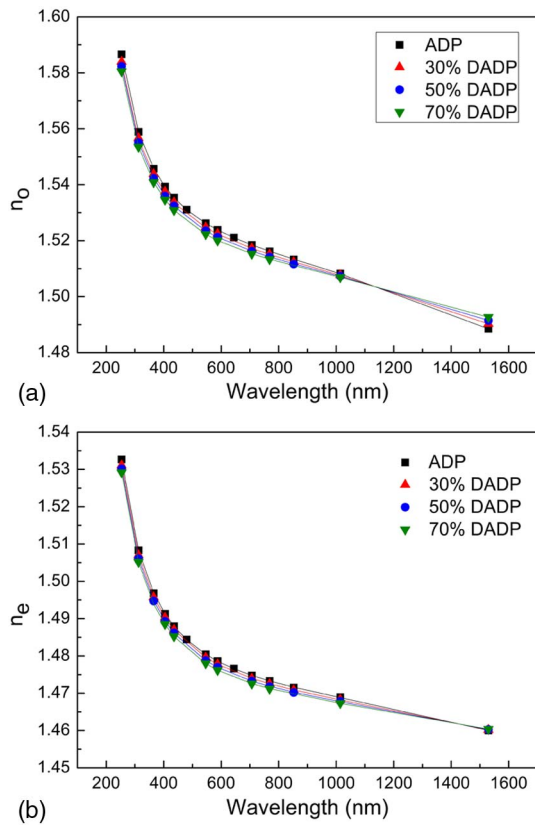


Fig. 4. Refractive indices of DADP crystals. (a) Ordinary indices of refraction. (b) Extraordinary indices of refraction. Points indicate experimental values whereas the curves are the fitting lines.

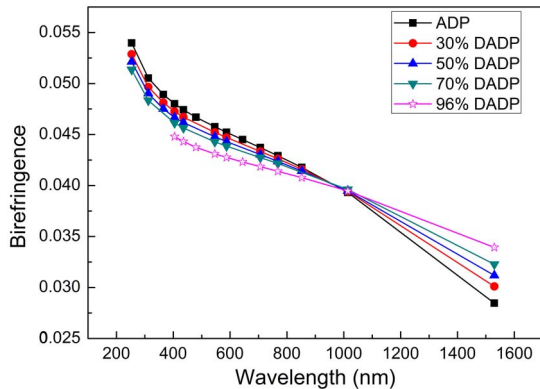


Fig. 5. Birefringence of DADP crystals. Data of 96% DADP comes from Kirby.

A modified version of the double-pole Sellmeier equation

$$n^2 = A + \frac{B\lambda^2}{\lambda^2 - C} + \frac{D}{\lambda^2 - E}, \quad (2)$$

where  $\lambda$  is the wavelength ( $\mu\text{m}$ ), and  $A$ ,  $B$ ,  $C$ ,  $D$ , and  $E$  are undetermined constants, was then used to fit the measured values. Equation (2) gives a good fit to the data and permits calculations of PM directions and NCPM wavelengths. The coefficients for the Sellmeier equation are given in Table 1.

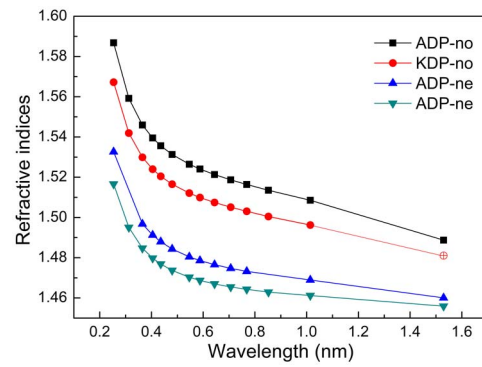


Fig. 6. Index comparisons of KDP and ADP. Last ordinary index of KDP is obtained by the extrapolation of the Sellmeier fit<sup>[10]</sup>.

Based on the data in Table 1, we have calculated the indices at relevant wavelengths for SHG and THG. The calculated PM angles are presented in Table 2. The deuterated crystals show smaller values than pure crystal especially at 1064 nm. With the increasing of deuterium content, the PM angles have obviously decreased. The variation in SHG process is more distinct than THG. Compared with ADP crystal, DADP crystal is more sensitive to the laser wavelength change. Thus, crystals with different deuterium contents should be processed into various directions when used in harmonic experiments, especially with different fundamental lasers.

The Type I NCPM at  $(90^\circ, 45^\circ)$  direction can be realized when

$$n_e(2\omega) = n_o(\omega) \quad (3)$$

The calculated values of NCPM wavelengths are shown in Table 3. To examine the accuracy of these results, we have processed several  $(90^\circ, 45^\circ)$ -cut crystal samples and measured the NCPM wavelengths on an OPO laser system. The experimental data are also listed in Table 3. The calculated NCPM wavelengths increased with deuterium content, which reveal the same trend with the experimental data. For DKDP crystals, the NCPM process of  $526 \rightarrow 263$  nm can be realized at 301 K with the deuterium content of 74% (80% in solution)<sup>[23]</sup>. For DADP crystals, this process can be realized at 302 K with obviously small deuterium content of about 40%. This can consequently save cost in the application of FHG. Considered the higher conversion efficiency and laser damage threshold, and the easy means of growing large-size crystals by rapid growth method, DADP crystals could be promising candidates in UV frequency conversion areas. It can be seen in Table 3 that the difference between the experimental value and calculated value of NCPM is less than 2 nm, mainly due to the different experiment temperature. The refractive indices were measured at 302 K while the NCPM wavelengths were measured at 292 K. Ji reported that the NCPM FHG process of 1053 nm laser can be realized by 60% DADP at 297 K<sup>[9]</sup>, which also corresponds to our results considering the slight

**Table 1.** Sellmeier Parameters of DADP Crystals

		<i>A</i>	<i>B</i>	<i>C</i>	<i>D</i>	<i>E</i>
ADP	$n_o$	2.29933	0.61290	18.52848	0.01143	0.01245
	$n_e$	2.16050	0.12999	11.53923	0.00991	0.01197
DADP, 30%	$n_o$	2.29541	1.10548	34.99480	0.01104	0.01266
	$n_e$	2.15862	0.23192	20.06127	0.00972	0.01222
DADP, 30%	$n_o$	2.29090	1.07025	37.56861	0.01104	0.01292
	$n_e$	2.15603	0.19362	18.70658	0.00965	0.01249
DADP, 70%	$n_o$	2.28573	0.58616	24.31843	0.01109	0.01251
	$n_e$	2.15355	0.15057	16.50826	0.00958	0.01268

**Table 2.** Calculated PM Angles for DADP Crystals

	SHG-I		SHG-II		THG-I		THG-II	
	1053	1064	1053	1064	1053	1064	1053	1064
ADP	41.31	41.34	60.77	60.71	48.30	47.87	60.79	60.05
DADP, 30%	40.35	40.35	59.45	59.35	47.87	47.42	60.49	59.73
DADP, 50%	39.35	39.33	57.94	57.80	47.58	47.13	60.32	59.55
DADP, 70%	38.21	38.15	56.26	56.08	47.26	46.78	60.12	59.32

**Table 3.** Calculated NCPM Wavelengths for DADP Crystals<sup>a</sup>

	ADP	30%	50%	70%
Experiment value (292 K)	524	524–525	525–526	—
Calculated value (302 K)	525.4	525.5	527.3	528.6

<sup>a</sup>Values are in nanometers.

variation of temperature and deuterium content. The consistency of experimental value and calculated value proved that the refractive indices and Sellmeier equations showed in this work is of good accuracy.

In conclusion, the variation of the refractive indices with deuterated content for DADP crystals is measured as a function of wavelength. The refractive indices decrease with the increasing wavelength and deuterated content. A modified version of the double-pole Sellmeier equation is used to fit the measured data. The Sellmeier equation gives a close fit to the data and permits a calculation of PM angles and NCPM wavelengths. The PM angles decrease with the deuterated content especially at SHG. The difference of PM angles between 1053 and 1064 nm laser wavelength also increase with the deuterated content. The calculated NCPM wavelength increases with the deuterated content which is consistent with the experimental trend. The agreement between calculation and experiment indicates the accuracy of refractive indices

measurements and fitting. DADP crystal can realize the FHG process in smaller deuterium content than DKDP. The PM characteristics together with other properties make DADP crystals promising substitutes in frequency conversion domains.

This work was supported by the National Natural Science Foundation of China (Nos. 51323002 and 51402173), the Independent Innovation Foundation of Shandong University (No. 2012JC016), the National Science Foundation for Distinguished Young Scholar of Shandong Province (No. JQ201218), and the Project supported by NPL and CAEP (No. 2014BB07).

## References

1. B. Liu, G. Hu, Q. Zhang, X. Sun, and X. Xu, *Chin. Opt. Lett.* **12**, 101604 (2014).
2. L. Ji, B. Zhu, C. Liu, T. Wang, and Z. Lin, *Chin. Opt. Lett.* **12**, 031902 (2014).
3. J. Reintjes and R. C. Eckardt, *Appl. Phys. Lett.* **30**, 91 (1977).
4. G. J. Linford, B. C. Johnson, J. S. Hildum, W. E. Martin, K. Snyder, R. D. Boyd, W. L. Smith, C. L. Vercimak, D. Eimerl, and J. T. Hunt, *Appl. Opt.* **21**, 3633 (1982).
5. D. A. Roberts, *IEEE J. Quantum Electron.* **28**, 2057 (1992).
6. S. Ji, F. Wang, L. Zhu, X. Xu, Z. Wang, and X. Sun, *Sci. Rep.* **3**, 1605 (2013).
7. V. S. Gorelik, A. A. Kaminskii, N. N. Melnik, P. P. Sverbil, Y. P. Voinov, T. N. Zavaritskaya, and L. I. Zlobina, *J. Russ. Laser Res.* **29**, 357 (2008).

8. A. A. Kaminskii, V. V. Dolbinina, H. Rhee, H. J. Eichler, K. Ueda, K. Takaichi, A. Shirakawa, M. Tokurakawa, J. Dong, and D. Jaque, *Laser Phys. Lett.* **5**, 532 (2008).
9. S. Ji, F. Wang, M. Xu, L. Zhu, X. Xu, Z. Wang, and X. Sun, *Opt. Lett.* **38**, 1679 (2013).
10. L. Zhu, X. Zhang, M. Xu, B. Liu, S. Ji, L. Zhang, H. Zhou, F. Liu, Z. Wang, and X. Sun, *AIP Adv.* **3**, 112114 (2013).
11. M. S. Pandian and P. Ramasamy, *Mater. Chem. Phys.* **132**, 1019 (2012).
12. M. S. Pandian, K. Boopathi, P. Ramasamy, and G. Bhagavannarayana, *Mater. Res. Bull.* **47**, 826 (2012).
13. M. S. Pandian and P. Ramasamy, *J. Cryst. Growth* **312**, 413 (2010).
14. H. Yin, Y. Liu, Z. Yu, Q. Shi, H. Gong, X. Wu, and X. Song, *Chin. Opt. Lett.* **11**, 101901 (2013).
15. F. Zernike, *J. Opt. Soc. Am.* **54**, 1215 (1964).
16. K. W. Kirby and L. G. DeShazer, *J. Opt. Soc. Am. B* **4**, 1072 (1987).
17. W. Liu, X. Yin, S. Wang, Z. Wang, J. Ding, Y. Sun, and G. Liu, *Opt. Laser Technol.* **44**, 1769 (2012).
18. R. A. Phillips, *J. Opt. Soc. Am.* **56**, 629 (1966).
19. N. P. Barnes and D. J. Gettemy, *J. Opt. Soc. Am.* **72**, 895 (1982).
20. D. Eimerl, *Ferroelectrics* **72**, 95 (1987).
21. A. Dyan, G. Duchateau, S. Eslava, J. L. Stehle, D. Damiani, and H. Piombini, *J. Mod. Opt.* **56**, 27 (2009).
22. R. D. Shannon and R. X. Fischer, *Phys. Rev. B* **73**, 235111 (2006).
23. S. Ji, S. Zhang, M. Xu, B. Liu, L. Zhu, L. Zhang, X. Xu, Z. Wang, and X. Sun, *Opt. Mater. Express* **2**, 735 (2012).